Journal of Electronic Imaging 18(1), 013012 (Jan–Mar 2009)

Shape-based hand recognition approach using the morphological pattern spectrum

Juan Manuel Ramirez-Cortes
National Institute for Astrophysics, Optics, and Electronics
Electronics Department
Tonantzintla, Puebla
72840, Mexico
E-mail: jmram@inaoep.mx

Pilar Gomez-Gil
National Institute for Astrophysics, Optics, and Electronics
Computer Science Department
Tonantzintla, Puebla
72840, Mexico

Gabriel Sanchez-Perez
Cesar Prieto-Castro
National Institute for Astrophysics, Optics, and Electronics
Electronics Department
Tonantzintla, Puebla
72840, Mexico

Abstract. *We propose the use of the morphological pattern spectrum, or pecstrum, as the base of a biometric shape-based hand recognition system. The system receives an image of the right hand of a subject in an unconstrained pose, which is captured with a commercial flatbed scanner. According to pecstrum property of invariance to translation and rotation, the system does not require the use of pegs for a fixed hand position, which simplifies the image acquisition process. This novel feature-extraction method is tested using a Euclidean distance classifier for identification and verification cases, obtaining 97% correct identification, and an equal error rate (EER) of 0.0285 (2.85%) for the verification mode. The obtained results indicate that the pattern spectrum represents a good feature-extraction alternative for low- and medium-level hand-shape-based biometric applications.*
 [DOI: 10.1117/1.3099712]

1 Introduction

Automatic personal identification and verification based on biometrics has received extensive attention in past years. A biometric system aims to provide automatic recognition of an individual based on features or characteristics unique to each human being. Biometric systems are based on several modalities, such as iris, voice, face, ear shape, hand shape, fingerprints, palm prints, or dynamical features like gait, on-line signature verification, and others.[1] Requirements, strengths, and weaknesses of each method have been widely reported in the literature.

Paper 08092RR received Jun. 10, 2008; revised manuscript received Jan. 29, 2009; accepted for publication Feb. 11, 2009; published online Mar. 19, 2009.

1017-9909/2009/18(1)/013012/6/$25.00 © 2009 SPIE and IS&T.

Among these modalities, hand-shape recognition has received significant attention due to its convenience in setup complexity, and its psychological acceptance as a noninvasive method, since it does not produce anxiety in the user as other techniques could.[2] However, hand-based biometric systems are limited to be commonly used in small- to medium-scale person verification applications, because geometric features of the hand are less distinctive than fingerprint or iris features.[3] In past years some commercial systems using this modality have been developed, and new algorithms have been proposed. Many hand-based biometric techniques use geometric features such as finger and palm heights, finger widths, palm-finger ratios,[4–6] palmprint information, palm contour, or a combination of palmprint features and geometric form measurements.[2,7] Several mathematical approaches for feature extraction have been proposed, such as Hausdorff distance,[8] B-spline curves,[9] geometric implicit polynomials,[10] or high-order Zernike moments.[3] Excellent references comparing different algorithms can be found in the literature.[3,11,12] We propose the use of the morphological operator *pecstrum* or *pattern spectrum*, as a novel feature extractor for a shape-based hand recognition system.

It is interesting to analyze the methods used in previous research on hand-shape segmentation. In most cases, input images are formed by the hand, wrist, and a portion of the forearm. Segmentation of the hand shape has been accomplished through several approaches. Amayeh *et al.*[3] detected the palm by finding the largest circle marked on the hand silhouette using morphological operators. Then, the

intersection of the forearm with the boundary of the circle is used to segment the hand shape. Fouquier *et al.*[5] performed hand-shape segmentation by drawing a wrist line based on geometrical considerations and *ad hoc* criteria related to the measurement of the largest palm width. Yoruk *et al.*[8] used two methods to synthesize a wrist boundary. The first approach was the implementation of a curve completion algorithm called the Euler spiral, which furnishes a natural completion of the hand-shape contour in the wrist part. Their second approach was simply a guillotine cut of the hand shape at the same latitudes determined by some specific points. In the work presented here, a setup with lateral light illumination placed under the arm of the subject was used. This style of lighting automatically eliminates the area corresponding to the wrist and the forearm directly during the acquisition process, which provides natural hand-shape segmentation with good results. It is important to point out that the method described in this work considers the input image as represented in hand-shape form, therefore to use it with other databases, preprocessing over the images is required.

2 Pattern Spectrum

Mathematical morphology is a geometric approach to nonlinear image processing that was developed as a powerful tool for shape analysis in binary and grayscale images.[13,14] Morphological operators are defined as combinations of basic numerical operations taking place over an image A and a small object B, called a *structuring element*. B can be seen as a probe that scans the image and modifies it according to some specified rule. The shape and size of B, which is typically much smaller than image A, in conjunction with the specified rule, define the characteristics of the performed process. An interesting morphological operator is the *pattern spectrum or pecstrum*. This operator decomposes the target image in morphological components according to the shape and size of the structuring element, providing a quantitative analysis of the morphological content of the image.[14,15] Pecstrum was originally developed by Pitas and Venetsanopoulus,[13] and Maragos.[16] Although it presents excellent properties as a shape extractor with invariance to translation and rotation, pecstrum has not been extensively used, probably because it is a computationally intensive algorithm. However, this drawback may be minimized using hardware implementations. Pecstrum has been used in the last few years with several applications: analysis of partial discharges in high voltage systems,[17] automatic recognition of automotive plates,[18] texture analysis using images of debris particles in polymers and composite materials,[19,20] and cytology of bone marrow images for the counting of white blood cells based on morphological granulometries.[21]

Binary-image mathematical morphology is based on two basic operators extensively presented in the literature known as *dilation* and *erosion* and defined respectively as:[13]

$$A \oplus B = \bigcup_{b \in B} A_b, \tag{1}$$

$$A \Theta B = \bigcap_{b \in B} A_{-b}. \tag{2}$$

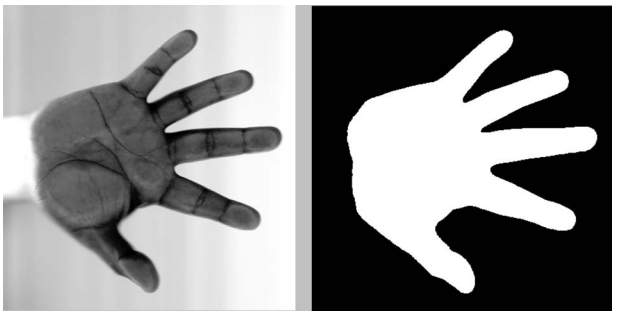

Fig. 1 Hand shape segmentation: grayscale-captured image and its corresponding binary segmented image.

The dilation and erosion of A by B are then regarded as the set *union* or *intersection*, respectively, of the objects A translated by all vectors contained in B. The backbone of the pattern spectrum is the *opening* morphological filter, defined as an erosion operation followed by a dilation using the same structuring element:

$$A \circ B = (A \Theta B) \oplus B. \tag{3}$$

In the opening operation, dilation attempts to undo erosion; however, some details closely related to shape and size of the structuring element will vanish. Furthermore, an object disappearing as a consequence of erosion cannot be recovered. In a pattern spectrum, the progressive vanishing of the image is numerically captured by measuring the differences in area in every step.

Formally, the pattern spectrum of a compact binary image $A \subseteq R^2$, relative to a convex binary pattern $B \subseteq R^2$, is defined as the differential size distribution function:

$$P_x(n,B) = \frac{dM(A \circ nB)}{dn} \quad n \geqslant 0. \tag{4}$$

M represents the area measured in the intermediate operations, and nB is the n-times dilated structuring element. The discrete form of the pattern spectrum is given by:

$$P(n,B) = \frac{M[A \circ nB] - M[A \circ (n+1)B]}{M[A]}. \tag{5}$$

Pecstrum has the property of invariance to translation and rotation when B is an isotropic structuring element. Scale is determined by the size of the structuring element.

3 Feature Extraction Using the Pattern Spectrum

The images used in this work were obtained from the right hand of subjects in an unconstrained pose, using a flatbed scanner at 50 dpi and reduced to a size of 256×256 pixels. The subjects were asked to stretch their hand naturally with their fingers separated, and to place it inside a square drawn in the scanner at a reasonable vertical hand position. Various hand positions with different extended angles between fingers were thus obtained. An *ad hoc* lateral light illumination pointed at the forearm of the subject was used to eliminate automatically the area corresponding to the wrist, as shown in Fig. 1. The palm shape was then segmented by simple binarization and contrast inversion, with a gray-level threshold method using an ex-

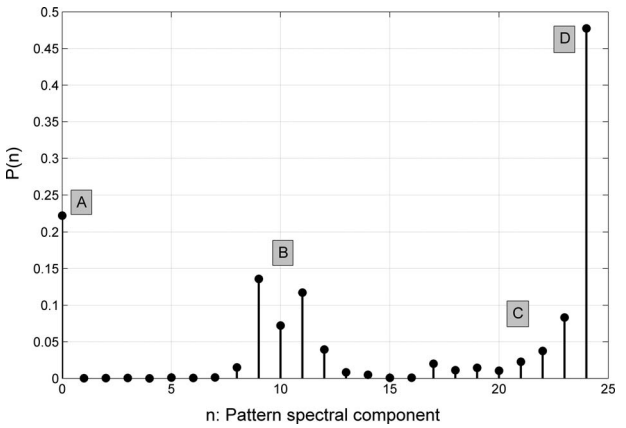

Fig. 2 Hand-shape feature vector based on the morphological pattern spectrum.

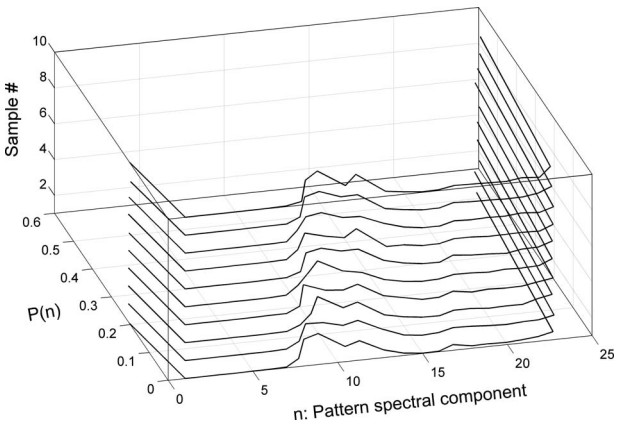

Fig. 4 Pattern spectra of ten samples from the same class.

perimentally determined threshold of 150, without additional processing. It was observed that no additional information about the hand shape was obtained in the last stages of pecstrum calculation, due to the tendency of the central part of the hand to approximate a round form, which produces pecstrum values near zero. Execution time of erosion and dilation operations increases exponentially with the size of the structuring element; therefore, computation of the pecstrum was optimized by doubling the step size of the structuring element in the last stages when half the area of the hand shape is surpassed. This adjustment allows the system to accelerate the execution time of the process without losing definition of the morphology definition of the palm shape, and avoiding an unnecessary increasing in the feature vector size.

Figure 2 shows a pecstrum-based feature vector obtained from the hand-shape image in Fig. 1. The structuring element is given by a disk with an incremental radius of one pixel per iteration. The first value plotted in Fig. 2 corresponds to the total area of the hand shape normalized to the window size, and the rest are values of the pattern spectrum obtained according to Eq. (5). The maximum vector size obtained was $n=25$, corresponding to the last iteration in which the image totally dissipates. A detailed description of the obtained feature vector plotted in Fig. 2 is as follows.

- The first value (labeled A) at $n=0$ corresponds to the total area of the image, normalized to the window size.

Fig. 3 Ten samples from the same subject with variations in the extended angle between fingers.

- The intermediate values located in the region labeled B reflect the morphological constitution of the fingers.
- The values in the region labeled C are related to the shape of the palm. Typically, a symmetric palm with a close-to-circle form gives small values in that region.
- The last value (labeled D) reflects the size of the central palm shape.

Intraclass samples included hand-shape images showing natural variations in the position of fingers. According to the obtained results, a pattern spectrum is able to tolerate finger displacements and hand rotations, and to extract a good representation of the morphological constitution of the hand shape. Figure 3 shows an example with a collection of ten samples obtained from the same subject (notice variations in finger positions). The corresponding pattern spectra are plotted in Fig. 4, and Fig. 5 shows the pattern spectra obtained from ten subjects belonging to different classes. To obtain an insight about the statistical data distribution, a basic analysis on inter- and intraclasses is reported in the next section.

Morphological operations are based on evaluating values contained in a local neighborhood of a pixel defined by a structuring element. For large neighborhoods, such calculations become computationally intensive. For the basic morphological functions of erosion and dilation, the num-

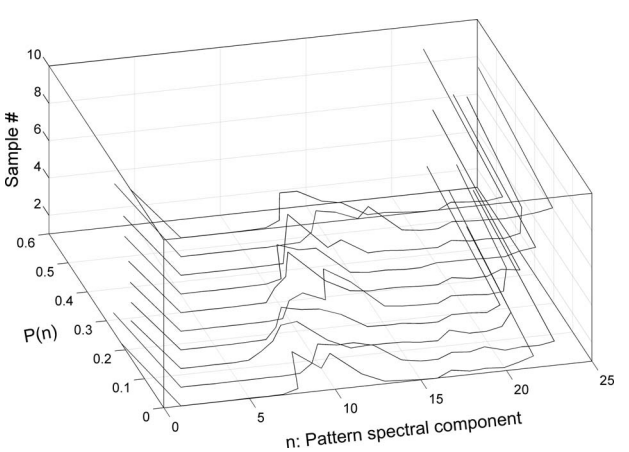

Fig. 5 Pattern spectra of ten samples from different classes.

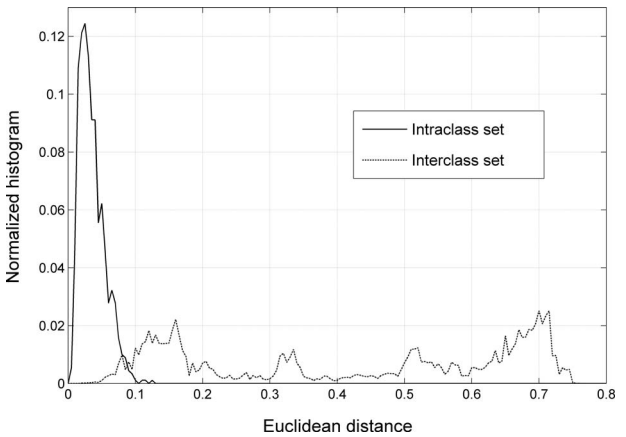

Fig. 6 Intraclass and interclass statistical distribution.

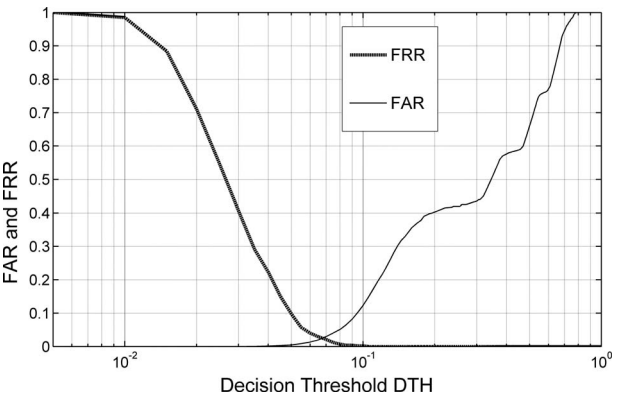

Fig. 7 Average false rejection rate and false acceptance rate curves.

ber of operations is proportional to the area of the structuring element. In this work, the structuring element is given by a circle with radius N_{SE} (SE stands for structuring element), so the complexity of each operation is proportional to $(N_{SE})^2$. The pattern spectrum involves several iterations of basic morphological operations with a structuring element of increasing size, and its complexity is proportional to $\Sigma_{N_{se}=1}^{m} 2(N_{SE})^2$, where m represents the value of the last iteration in which the image totally dissipates.

The experiments reported in this work were carried out using Matlab 7.0. We are currently pursuing an optimized hardware implementation of the pattern spectrum based on field programmable gate arrays (FPGAs),[22,23] which would be required to make a practically exploitable prototype, based on the methodology described here.

4 Experimental Description and Results

We collected 400 images of the right hand, 10 samples from each subject, with a total of 40 subjects. To evaluate this method, some experiments based on Euclidean distances were performed. The maximum distance between samples was 0.8021. The average distance between mean classes was 0.469758. Our proposed feature vector led samples belonging to the same subject to be located in clusters with an average mean distance and standard deviation of 0.04468 and 0.01265, respectively. Figure 6 shows the normalized histograms for intraclass and interclass sets, which represent the probability distribution functions of the Euclidean distances within samples in the database. The intraclass set consists of distance pairs within the clusters of the same subject. The interclass set corresponds to the pairing of distances from different classes. As expected, the intraclass distribution is clustered toward the origin, whereas the interclass distance distribution is scattered and away from the origin.

The system performance was evaluated in two different modes: identification and verification. For the identification case, the system was trained using patterns of several persons, and a biometric template was calculated for each subject. The pattern under test was matched against every template built by the system through the Euclidean distance, and the system assigned the pattern to the person with the most similar template (smallest Euclidean distance). To perform a two-fold cross-validation process, the database was divided into two groups with five samples per subject in each group. The first group was used as an enrollment template, while the second group was used for the authentication process. The experiment was repeated ten times, using a random enrollment template. An average identification rate of 97% was obtained while using this minimum Euclidean distance classifier.

In the verification mode, the system performance was evaluated through the false acceptance rate (FAR) and false rejection rate (FRR). The FAR is a measure of the likelihood that the system will incorrectly accept an access attempt by an unauthorized user, and it is stated as the ratio of the number of false acceptances divided by the number of attempts. On the other hand, the FRR is the measure of the likelihood that the system will incorrectly reject an access attempt by an authorized user, and it is stated as the ratio of the number of false rejections divided by the number of attempts. These two rates exhibit a tradeoff that can be controlled by a decision threshold (DTH). This threshold represents the Euclidean distance, which establishes the separation point between the matching and nonmatching accesses. The equal error rate (EER) is defined as the point at which FRR and FAR exhibit the same value. Figure 7 shows the average FAR and FRR curves obtained for a population of $N=40$ through a two-fold cross-validation process. In a biometric system, performance is usually analyzed through a receiver operation characteristic plot (ROC), which represents the operating points of the system. The ROC curve is obtained from the FRR and FAR curves by moving DTH across the range of the decision threshold. Figure 8 shows the average ROC curves in logarithmic scales, which have been obtained through experiments with several database populations. In the case corresponding to $N=40$, an equal error rate (EER) of 0.0285 was obtained at a decision threshold of DTH=0.068.

Table 1 provides a comparison of the system performance obtained from different approaches that are reported in the literature.[24–28] Although a direct comparison is not possible due to the differences in database size, number of samples per subject, and feature extraction methodology, it is evident that the results obtained are very competitive. Further research incorporating additional modalities will be carried out. Specifically, separate morphological analysis of

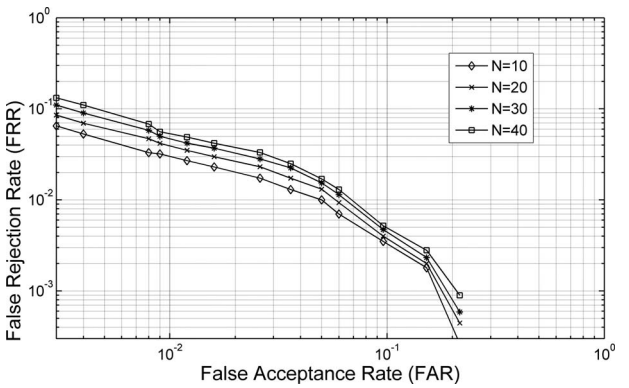

Fig. 8 Average receiver operation characteristic curves (ROC).

each finger previously segmented and a further numerical integration should provide a detailed and presumably more precise hand-shape representation, according to results reported in the literature.[5,28,29]

5 Conclusions

A novel hand-shape feature extraction based on the morphological pattern spectrum is presented for biometric applications. The results obtained indicate that the pattern spectrum represents a good choice of feature extraction methodology for low- and medium-scale applications. The method is tested on a database of 40 subjects using an Euclidean distance classifier, obtaining an average identification rate of 97%, and an average EER=0.0285 (2.85%) for the verification mode. These results are very competitive when they are compared with systems previously reported in the literature,[3,11,12] although experiments with larger databases are needed. A FPGA implementation of the described algorithm is currently under construction in our research group, aiming for the construction of a prototype for real-time biometry. Further experimentation with other recognition methods such as neural network-based classifiers, support vector machines, and other approaches on larger databases is currently in progress in our research group.

Table 1 Comparison of several reported methods.

Reference number	Number of subjects	Number of samples per subject	Features	Classification approach	Performance
24	20	10	Geometric features	Euclidean, Hamming, Gaussian mixture models (GMM)	EER=0.06 with GMM
25	22	12	Geometric features and fingertip regions	GMM	FAR=0.022 FRR=0.1111
26	130	5	Geometric features	Euclidean distance	FAR=0.153 FRR=0.13
9	20	6	B-spline curves, thumb length, and palm width	Minimum distance between a point and a B-spline curve	EER=0.05
27	70	10	30 geometric features	Nearest box and Euclidean ball	FAR=0.01 FRR0.03
28	108	5	Geometric features. Width of fingers at several points.	Distance between width feature vectors	EER up to 0.0241
3	40	10	Zernike moments	Euclidean distance	FAR=0.01 FRR=0.0242 EER=0.0164
7	100	10	Geometric features and hand area	Normalized correlation	FRR=0.0834 when FAR=0.01
5	750	3/6	Finger geometry measurements	Symmetric Kullback-Leibler distance	EER=0.0421
This work	40	10	Morphological pattern spectrum	Euclidean distance	FRR=0.052 when FAR=0.01 EER=0.0285

Acknowledgment

The authors would like to thank the anonymous reviewers for their detailed and helpful comments.

References

1. *Handbook of Biometrics*, A. K. Jain, P. Flynn, and A. Ross, Eds., Springer, Berlin (2007).
2. E. Yoruk, H. Dutagaci, and B. Sankur, "Hand biometrics," *Image Vis. Comput.* **24**, 483–497 (2006).
3. G. Amayeh, G. Bebis, A. Erol, and M. Nicolescu, "Peg-free hand shape verification using high order Zernike moments," *Proc. IEEE Conf. Computer Vision Patt. Recog. Workshop*, pp. 40–48 (2006).
4. C. L. Su, "Hand image recognition by the techniques of hand shape scaling and image weight scaling," *Expert Syst. App.* **34**, 2976–2987 (2008).
5. G. Fouquier, L. Likforman, J. Darbon, and B. Sankur, "The biosecure geometry-based system for hand modality," *Proc. IEEE ICASSP*, I801–I804 (2007).
6. B. Yaroslav, J. Sachin, K. Piyush, and S. Saurabh, "Hand recognition using geometric classifiers," *Proc. Intl. Conf. Biometric Authent.*, pp. 753–760 (2004).
7. D. C. M. Kumar, H. C. Shen, and A. K. Jain, "Personal authentication using hand images," *Pattern Recogn. Lett.*, **27**, 1478–1486 (2006).
8. E. Yoruk, E. Konukoglu, B. Sankur, and J. Darbon, "Shape-based hand recognition," *IEEE Trans. Image Process.* **15**(7), 1803–1815 (2006).
9. Y. Liang, M. F. Pollik, and W. T. Hewitt, "Using B-spline curves for hand recognition," *Proc. IEEE Intl. Conf. Patt. Recog.*, pp. 274–277 (2004).
10. C. Oden, A. Ercil, and B. Buke, "Combining implicit polynomials and geometric features for hand recognition," *Pattern Recogn. Lett.*, **24**, 2145–2152 (2003).
11. H. Dutagaci, B. Sankur, and E. Yoruk, "Comparative analysis of global hand appearance-based person recognition," *J. Electron. Imaging* **17**(1), 1801–1819 (2008).
12. A. Mitome and R. Ishii, "A comparison of hand shape recognition algorithms," *Proc. IEEE Ann. Conf. Ind. Elec. Soc.*, pp. 2261–2265 (2003).
13. A. Pitas and A. N. Venetsanopoulus, *Non-linear Digital Filters; Principles and Applications*, Kluwer Academic Publisher, Norwell, MA (1990).
14. A. Ledda, J. Quintelier, P. Samyn, P. Baets, and W. Phillips, "Quantitative image analysis with mathematical morphology," *ProRISC Ann. Workshop Circuits, Syst. Signal Process.*, pp. 399–406 (2000).
15. A. Ledda and W. Phillips, "Majority ordering and the morphological pattern spectrum," *Conf. Proc. Adv. Concepts Intelli. Vision Syst.*, pp. 356–363 (2005).
16. P. Maragos, "Pattern spectrum and multi-scale shape representation," *IEEE Trans. Pattern Anal. Mach. Intell.*, **11**, 701–716 (1989).
17. L. Yun-Peng, L. Fang-Cheng, and L. Cheng-Rong, "Pattern recognition of partial discharge based on its pattern spectrum," *Proc. Intl. Symp. Electric. Insul. Mat.* 763–766 (2005).
18. A. Valderrabano, D. Baez, and J. M. Ramirez, "Pattern recognition in automotive plates," *Proc. Midwest Symp. Circuits Syst.* 314–317 (1998).
19. A. Asano, "Texture analysis using morphology pattern spectrum and optimization of structuring element," *Proc. Intl. Conf. Image Anal. Process.*, pp. 209–215 (1999).
20. Ledda, P. Samyn, J. Quintelier, P. D. Baets, and W. Phillips, "Polymer analysis with mathematical morphology," *Proc. IEEE Benelux Signal Process. Symp.*, pp. 87–92 (2004).
21. N. Theera-Umphon and S. Dhompongsa, "Morphological granulometric features of nucleus in automatic bone marrow white blood cell classification," *IEEE Trans. Inf. Technol. Biomed.* **11**(3), 353–359 (2007).
22. J. Velten and A. Kummert, "FPGA based implementation of variable sized structuring elements for 2-D binary morphological operations," *Proc. First IEEE Intl. Workshop Electron. Design, Test. Appl.*, pp. 309–312 (2002).
23. H. Hedberg, F. Kristensen, and V. Owall, "Low-complexity binary morphology architectures with flat rectangular structuring elements," *IEEE Trans. Circuits Syst., I: Regul. Pap.*, **55**(8), 2216–2225 (2008).
24. R. Sanchez-Reillo, C. Sanchez-Avila, and A. Gonzalez-Marcos, "Biometric Identification through hand geometry measurements," *IEEE Trans. Pattern Anal. Mach. Intell.* **22**(10), 1168–1171 (2000).
25. A. L. N. Wong and P. Shi, "Peg free hand geometry recognition using hierarchical geometry and shape matching," *IAPR Workshop Machine Vision App.*, pp. 281–284 (2002).
26. S. Ribaric, D. Ribaric, and N. Pavesic, "Multimodal biometric user-identification system for network-based applications," *IEE Proc. Vision, Image, Signal Process.*, **50**(6), 409–416 (2003).
27. Y. Bulatov, S. Jambawalikar, P. Kumar, and S. Sethia, "Hand recognition using geometric classifiers," *Proc. First Intl. Conf. Biometric Authenti.*, pp. 753–759 (2004).
28. W. Xiong, C. Xu, and S. H. Ong, "Peg-free human hand shape analysis and recognition," *Proc. IEEE ICASSP*, pp. 77–80 (2005).
29. W. Xiong, K. Toh, W. Yau, and X. Jiang, "Model-guided deformable hand shape recognition without positioning aids," *Pattern Recogn.* **38**, 1651–1664 (2005).

Juan Manuel Ramirez-Cortes received the BSc degree from the National Polytechnic Institute, Mexico, the MSc degree from the National Institute of Astrophysics, Optics, and Electronics (INAOE), Mexico, and the PhD degree from Texas Tech University, all in electrical engineering. He is currently a Titular Researcher at the Electronics Department, INAOE, in Mexico. His research interests include signal and image processing, biometry, neural networks, fuzzy logic, and pattern recognition. He is a senior member of IEEE.

Pilar Gomez-Gil received the BSc degree from the *Universidad de las Americas AC*, Mexico, and the MSc and PhD degrees from Texas Tech University, all in computer science. She is currently an associate researcher in computer science at INAOE, Mexico. Her research interests include neural networks, signal processing, pattern recognition, and software engineering. She is a senior member of IEEE and a member of ACM.

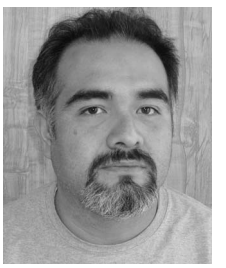

Gabriel Sanchez-Perez received the BSc degree in computer science, and the PhD degree in electronics and communications from the National Polytechnic Institute, Mexico. From 2001 to 2006, he was an assistant professor with the computer engineering department at the National Polytechnic Institute. In 2006 he joined the Graduate School of the National Polytechnic Institute of Mexico, where he is currently a professor. He is a member of IEEE and a member of the National Research System of Mexico.

Cesar Prieto-Castro received the BSc degree in electronics and communications engineering from *Instituto Tecnologico Superior de Jalapa*, Veracruz, Mexico, in 2007. He is currently working toward the MSc degree in electrical and computing engineering at the National Institute of Astrophysics, Optics, and Electronics, Mexico. His interests include digital signal and image processing, biometry, and data compression.